Chinese Chemical Letters 35 (2024) 108683

Contents lists available at ScienceDirect

Chinese Chemical Letters

journal homepage: www.elsevier.com/locate/cclet

Elaborately engineering of lipid nanoparticle for targeting delivery of siRNA and suppressing acute liver injury

Qiu Wang[a,1], Qikun Jiang[a,1], Dan Li[a], Zimeng Yang[a], Lin Gao[a], Fan Liu[a], Chang Li[a], Yao Feng[b], Zhonggui He[a], Cong Luo[a,*], Jin Sun[a,*]

[a] Department of Pharmaceutics, Wuya College of Innovation, Shenyang Pharmaceutical University, Shenyang 110016, China
[b] Kangya of Ningxia Pharmaceutical Co. Ltd., Yinchuan 750000, China

ARTICLE INFO

Article history:
Received 2 March 2023
Revised 7 June 2023
Accepted 11 June 2023
Available online 17 June 2023

Keywords:
Lipid nanoparticle
Targeting siRNA delivery
Acute liver injury
Gene silencing
Tumor necrosis factor α

ABSTRACT

Small interfering RNA (siRNA)-based gene silencing has been considered as a potential therapy modality against inflammatory diseases. Nevertheless, the effective delivery of siRNA to desired destination still remains challenging due to poor stability, high molecular weight and negative charge. Currently, ionizable lipid nanoparticle (LNP) has been extensively used as vector for effective delivery of siRNA. Herein, we report a mannose-modified LNP (M-MC3 LNP@TNFα) loading tumor necrosis factor α (TNFα) siRNA for targeting liver macrophages, achieving effectively inhibit acute liver injury. The M-MC3 LNP@TNFα not only increases the internalization of LNP by macrophages, but also enhances the gene silencing efficiency of TNFα *in vitro*. Additionally, the M-MC3 LNP@TNFα exhibits higher accumulation in liver of healthy mice than that of MC3 LNP@TNFα (un-modified LNP) owing to the targeting effect of mannose. As expected, the M-MC3 LNP@TNFα significantly suppresses the expression of TNFα and ameliorates liver damage in acute liver injury model. Such a LNP targeting siRNA delivery holds great potential for the treatment of diseases associated with liver in the future.

Acute liver injury presents an inflammatory disease, which is caused by a variety of etiologies such as drug poisoning, viral infection and alcohol abuse [1,2]. Tumor necrosis factor α (TNFα), one of the important pro-inflammatory factors, overproduced by liver macrophages is prominently associated with the pathogenesis of acute liver injury [1–4]. At present, TNFα monoclonal antibodies and small molecule inhibitors have been applied to intervene acute liver injury in clinical practice [3]. Unfortunately, these therapeutic approaches usually suffer from some undesired side effects and autoimmunity due to poor targeting ability of liver macrophages [3]. Therefore, it is essential to explore novel strategies to improve the therapeutic safety and effectiveness against acute liver injury.

Small interfering RNA (siRNA), a tool for gene silencing, can specifically degrade target mRNA and suppress gene expression [5–8]. The siRNA-based therapeutic modalities are regarded as promising for treating various diseases including genetic diseases, inflammatory diseases and cancer, *etc*. [9–13]. However, the clinical application of naked siRNA is bottlenecked due to its instability, poor cellular internalization and endosomal entrapment [1,3,10]. To circumvent above impediments, a series of vectors have been developed to improve the delivery efficiency of siRNA such as polymer, dendrimer, inorganic and lipid nanoparticles [14–21]. Among them, lipid nanoparticle (LNP) has been regarded as most potent delivery system owing to high cellular uptake, low immunogenicity and mature industrial manufacture technology [1,22]. For instance, the ionizable lipid material (dioleoyl-4-methyl-dimethylaminobutyric acid ester, DLin-MC3-DMA) approved by Food and Drug Administration (FDA) is used to wrap siRNA for fighting hereditary transthyretin mediated amyloidosis (hATTR) in clinic [23–25]. However, the targeting ability of DLin-MC3-DMA to liver macrophages is poor due to the lack of target. Currently, it has been covered that mannose receptor are highly expressed on the surface of macrophages [23,26]. In view of the above findings, mannose-targeted LNP is extraordinarily promising for enhancing the therapeutic effect of diseases based on liver macrophages.

Herein, we designed a mannose-modified TNFα-siRNA loaded LNP (M-MC3 LNP@TNFα) for targeting liver macrophages, silencing TNFα expression and treating acute liver injury (Fig. 1). The M-MC3 LNP@TNFα increased the targeting ability of liver macrophages of LNP with the aid of mannose, enhancing the accumulation of LNP in the liver. More importantly, M-MC3 LNP@TNFα exhibited better anti-inflammatory effect in acute liver injury

* Corresponding authors.
E-mail addresses: luocong@syphu.edu.cn (C. Luo), sunjin@syphu.edu.cn (J. Sun).
[1] These authors contributed equally to this work.

https://doi.org/10.1016/j.cclet.2023.108683
1001-8417/

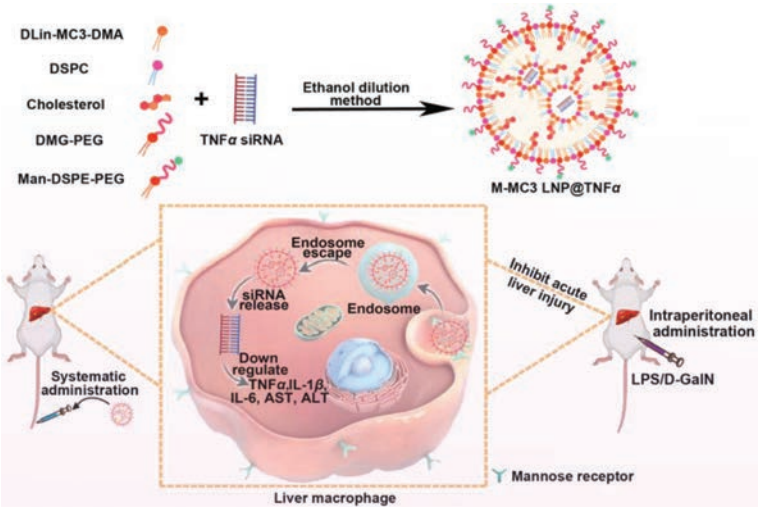

Fig. 1. Schematic representation the preparation process and anti-inflammatory effect of M-MC3 LNP@TNFα against mice with acute liver injury. The M-MC3 LNP@TNFα was constructed by using ethanol dilution method. The surface of LNP was modified with Man-DSPE-PEG to target mannose receptor of liver macrophages. After systemic administration of M-MC3 LNP@TNFα to targeted liver macrophages, LNP escaped from lysosomes and released TNFα siRNA into the cytoplasm, reducing the levels of TNFα, IL-6, IL-1β, AST and ALT.

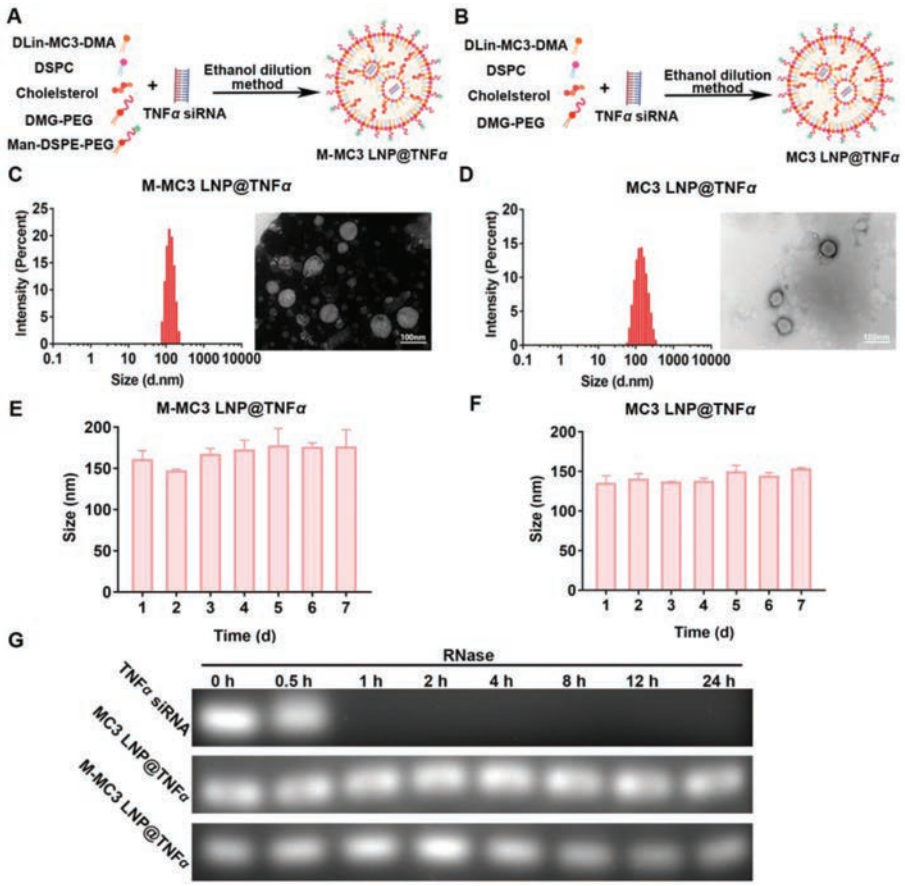

Fig. 2. Characterization of MC3 LNP@TNFα and M-MC3 LNP@TNFα *in vitro*. (A, B) Preparation process of M-MC3 LNP@TNFα and MC3 LNP@TNFα by using ethanol dilution. (C) Particle size distribution profile and TEM image of M-MC3 LNP@TNFα. (D) Particle size distribution profile and TEM image of MC3 LNP@TNFα, Scale bar: 100 nm. (E, F) The storage stability of M-MC3 LNP@TNFα and MC3 LNP@TNFα in 4 °C for 7 d, respectively. Data are presented as mean ± standard deviation (SD) ($n = 3$). (G) The stability of MC3 LNP@TNFα and M-MC3 LNP@TNFα in the presence of RNase within 24 h.

model compared with the MC3 LNP@TNFα. Such LNP-based gene therapy provides a promising strategy for treating liver-related diseases in future clinical applications.

Three TNFα siRNA sequences were devised to screen out the highest gene silencing efficiency by using TNFα enzyme linked immunosorbent assay (ELISA) kit. The siRNAs of different sequences were shown in the Table S1 (Supporting information). Among them, the named 631 TNFα siRNA sequence exhibited much higher gene silencing efficiency *in vitro* and *in vivo* than the other two sequences (Figs. S1 and S2 in Supporting information). Hence, 631 TNFα siRNA was selected as the optimal gene sequence for further investigation.

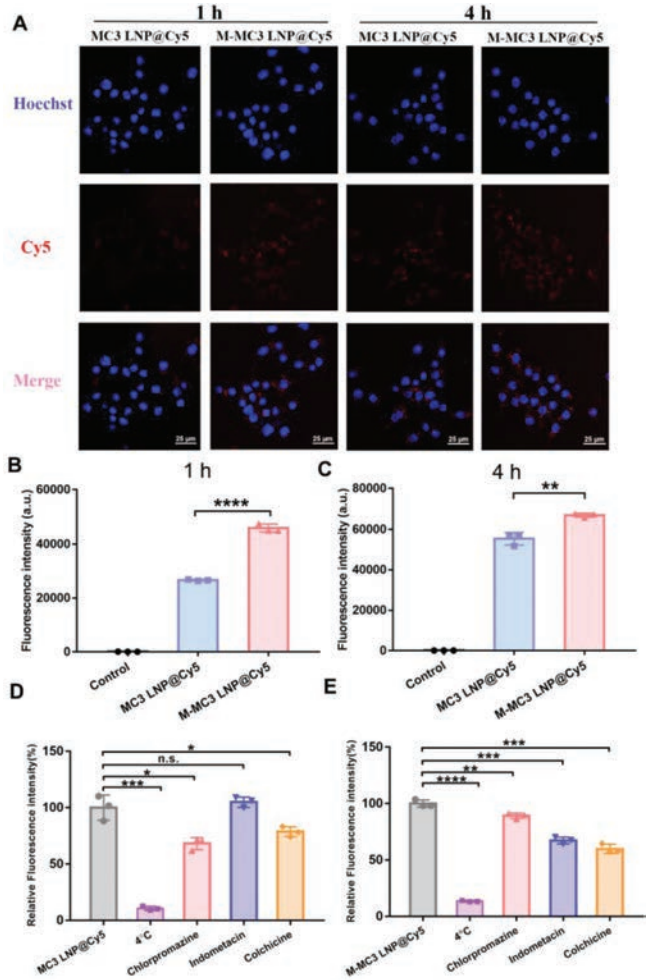

Fig. 3. *In vitro* cellular internalization and uptake mechanism of M-MC3 LNP@Cy5. (A) Confocal imaging of MC3 LNP@Cy5 and M-MC3 LNP@Cy5 in RAW 264.7 cells at both 1 h and 4 h (Scale bar: 25 μm). (B, C) The flow cytometry of RAW 264.7 cells after incubation with MC3 LNP@Cy5 and M-MC3 LNP@Cy5 at 1 h and 4 h, respectively. (D, E) The cellular uptake mechanism of MC3 LNP@Cy5 and M-MC3 LNP@Cy5, respectively. Data are presented as mean ± SD ($n = 3$, n.s.: no significance. $^{*}P < 0.05$, $^{**}P < 0.01$, $^{***}P < 0.001$, $^{****}P < 0.0001$).

The M-MC3 LNP@TNFα was prepared according to the ethanol dilution method reported in the literature [27]. The schematic illustration of the preparation process was shown in Fig. 2A. The size, polydispersity index (PDI) and encapsulation efficiency (EE) of M-MC3 LNP@TNFα with carriers of different molar ratios were exhibited in Table S2 (Supporting information). On the basis of above results, the M-MC3 LNP@TNFα with 1% Man-DSPE-PEG was served as optimal formulation owing to proper particle size and higher EE. In addition, the LNP without mannose modification (MC3 LNP@TNFα) was also constructed as control (Fig. 2B). As illustrated in Figs. 2C and D, the results of transmission electron microscope (TEM) and dynamic light scattering (DLS) showed that M-MC3 LNP@TNFα and MC3 LNP@TNFα had uniform spherical structures with average particle diameter of approximately 160 nm and 130 nm, respectively. And the zeta potentials of M-MC3 LNP@TNFα and MC3 LNP@TNFα were ∼+13.6 mV (Fig. S3 in Supporting information) and ∼+11.6 mV (Fig. S4 in Supporting information), respectively. Besides, the particle sizes of M-MC3 LNP@TNFα and MC3 LNP@TNFα were barely changed after 5 days storage at 4 °C, indicating the good storage stability (Figs. 2E and F). Furthermore, the agarose gel electrophoresis was applied to evaluate the TNFα siRNA degradation of LNPs under the action of RNase. As

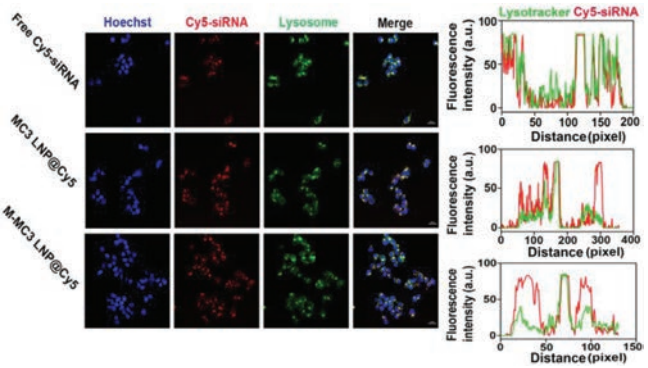

Fig. 4. Fluorescence imaging about colocalization of lysosome and Cy5-siRNA of MC3 LNP@Cy5 and M-MC3 LNP@Cy5 (Scale bar: 25 μm).

shown in Fig. 2G, the naked TNFα siRNA completely degraded in 1 h. However, the siRNA of MC3 LNP@TNFα and M-MC3 LNP@TNFα barely degraded within 24 h. These results demonstrated that MC3 LNP@TNFα and M-MC3 LNP@TNFα had good stability, which could inhibit the degradation of siRNA for longer time. *In vitro* drug release of LNPs in different pH conditions was explored by microplate reader. As exhibited in Fig. S5 (Supporting information), the release rate of siRNA from MC3 LNP@Cy5 and M-MC3 LNP@Cy5 was faster in pH 7.4 phosphate buffer saline (PBS) than that in pH 5.0 PBS. About 20% of siRNA was released from MC3 LNP@Cy5 and M-MC3 LNP@Cy5 within 12 h under neutral condition, while approximately 30% siRNA was released under acidic condition. These results revealed that the LNPs had acid-sensitive release characteristics due to the protonation effect of tertiary amino group in MC3.

The TNFα gene silencing efficiency of MC3 LNP@TNFα and M-MC3 LNP@TNFα in RAW 264.7 cells stimulated with lipopolysaccharide (LPS) was accessed by ELISA kit, Western blot and qPCR. As illustrated in Fig. S6 (Supporting information), compared with control and free TNFα siRNA, the MC3 LNP@TNFα and M-MC3 LNP@TNFα significantly inhibited the secretion of TNFα. Additionally, MC3 LNP@TNFα and M-MC3 LNP@TNFα not only downregulated TNFα expression, but also markedly reduced the TNFα mRNA levels in RAW 264.7 cells (Figs. S7 and S8 in Supporting information). Notably, M-MC3 LNP@TNFα demonstrated higher gene silencing efficiency than MC3 LNP@TNFα. These above results implied that mannose-modified LNPs could improve siRNA gene silencing efficiency owing to the binding effect of ligands-receptors of mannose.

The cellular internalization of MC3 LNP and M-MC3 LNP in RAW 264.7 cells at different time point was assessed by laser scanning confocal microscopy (CLSM). As exhibited in Fig. 3A, Cy5-labled siRNA presented red fluorescence in cytoplasm. Compared with MC3 LNP@Cy5, the M-MC3 LNP@Cy5 showed much stronger red fluorescent signal at both 1 h and 4 h, indicating that the M-MC3 LNP@Cy5 had higher cellular internalization efficiency. In addition, the semi-quantitative analysis of cellular uptake of M-MC3 LNP@Cy5 was also explored by using flow cytometry. As depicted in Figs. 3B and C, the M-MC3 LNP@Cy5 exhibited higher cellular uptake profile than that of MC3 LNP@Cy5, which was ascribed to the binding of mannose receptor-ligand. The results of semi-quantitative analysis were consistent with those of CLSM. Furthermore, the above results demonstrated that mannose-modified lipid could significantly improve the uptake of LNP in cells expressing mannose receptor.

Additionally, flow cytometry was employed to explore the internalization pathway of MC3 LNP@Cy5 and M-MC3 LNP@Cy5. It has been reported that extracellular nanoparticles are mainly internalized by cells *via* clathrin, caveolae and macropinocytosis-mediated

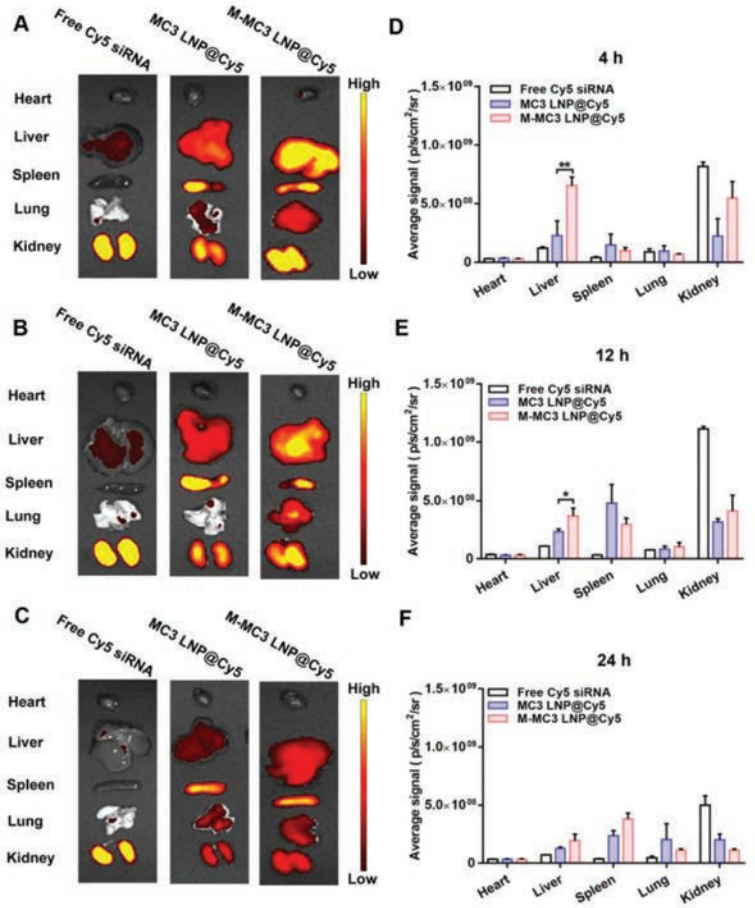

Fig. 5. The biodistribution of MC3 LNP@Cy5 and M-MC3 LNP@Cy5 in C57BL/6 mice. *Ex vivo* fluorescence imaging of heart, liver, spleen, lung and kidney at 4 h (A), 12 h (B) and 24 h (C); Semi-quantitative analysis of fluorescence intensity at 4 h (D), 12 h (E), 24 h (F). Data are presented as mean ± SD ($n = 3$, $^{*}P < 0.05$, $^{**}P < 0.01$).

endocytosis. As depicted in Fig. 3D, compared with cells without inhibitors treatment, the Cy5 fluorescence intensity of cells treated with chlorpromazine and colchicine decreased significantly. Similarly, the Cy5 fluorescence intensity of cells treated with three inhibitors also declined dramatically (Fig. 3E). These results demonstrated that the uptake pathway of MC3 LNP@Cy5 was dominantly mediated by clathrin and micropinocytosis, while the internalization of M-MC3 LNP@Cy5 mainly depended on clathrin, caveolin and micropinocytosis. Moreover, the fluorescence intensity of cells at 4 °C was extremely low, indicating that the uptake of MC3 LNP@Cy5 and M-MC3 LNP@Cy5 was rigorously energy-dependent.

The lysosome escape of siRNA is of vital significance for the gene silencing efficiency. Hence, the lysosomal escape ability of free Cy5-siRNA, MC3 LNP@Cy5 and M-MC3 LNP@Cy5 was investigated by CLSM. As depicted in Fig. 4, free Cy5-siRNA had strong co-localization with lysosome, almost all of which accumulated in lysosome. However, the siRNA of MC3 LNP@Cy5 and M-MC3 LNP@Cy5 had obvious lysosomal escape effect due to the protonation of tertiary amine structure of MC3 under acid conditions in lysosome and disturbance effect of long-chain alkyl of MC3 on lysosomal membrane. Moreover, the Pearson's correlation coefficient of lysosome and different formulations was calculated to observe lysosomal escape effect of LNPs more intuitively. The Pearson's coefficient is closer to 1, the worse the lysosomal escape effect. As shown in Fig. S9 (Supporting information), the Pearson's coefficient indicated that MC3 LNP@Cy5 and M-MC3 LNP@Cy5 had good lysosomal escape effect.

The cytotoxicity of MC3 LNP@TNFα and M-MC3 LNP@TNFα against RAW 264.7 cells was evaluated by MTT analysis. As illustrated in Fig. S10 (Supporting information), the cell viability of RAW 264.7 cells incubated with MC3 LNP@TNFα and M-MC3 LNP@TNFα was close to 100% in the concentration range from 2 ng/mL to 100 ng/mL, revealing that the above two LNPs had good biosafety for cells.

To investigate the targeting ability of M-MC3 LNP and MC3 LNP in liver, the test of tissue biodistribution was conducted in healthy C57BL/6 by using In Vivo Imaging Systems (IVIS). All animal experiments were approved by Animal Ethics Committee of Shenyang Pharmaceutical University. As illustrated in Figs. 5A–C, compared with MC3 LNP@Cy5 and M-MC3 LNP@Cy5, the Cy5-labeled siRNA showed higher fluorescent intensity in kidney due to the renal excretion of un-encapsulated siRNA. Moreover, it was observed that M-MC3 LNP@Cy5 exhibited dramatically higher fluorescence in liver than that of MC3 LNP@Cy5 at 4 h, 12 h and 24 h post-administration, implying higher accumulation of M-MC3 LNP@Cy5 in liver. The above results indicated that mannose-modified LNP could enhance the accumulation of siRNA in the liver, which was ascribed to good targeting ability of mannose to macrophages. Furthermore, it was also found that M-MC3 LNP@Cy5 and MC3 LNP@Cy5 exhibited stronger fluorescent intensity in liver at 4 h post-administration, the fluorescent intensity decreased gradually from 4 h to 24 h. The fluorescence semi-quantitative analysis results of tissue distribution at different time intervals were exhibited in Figs. 5D–F.

The acute liver injury animal model was constructed by intraperitoneal injection of LPS/D-GalN to induce TNFα secretion in liver of C57BL/6 mice. LPS is the main component of the outer wall of Gram-negative bacteria, which can trigger inflammatory cy-

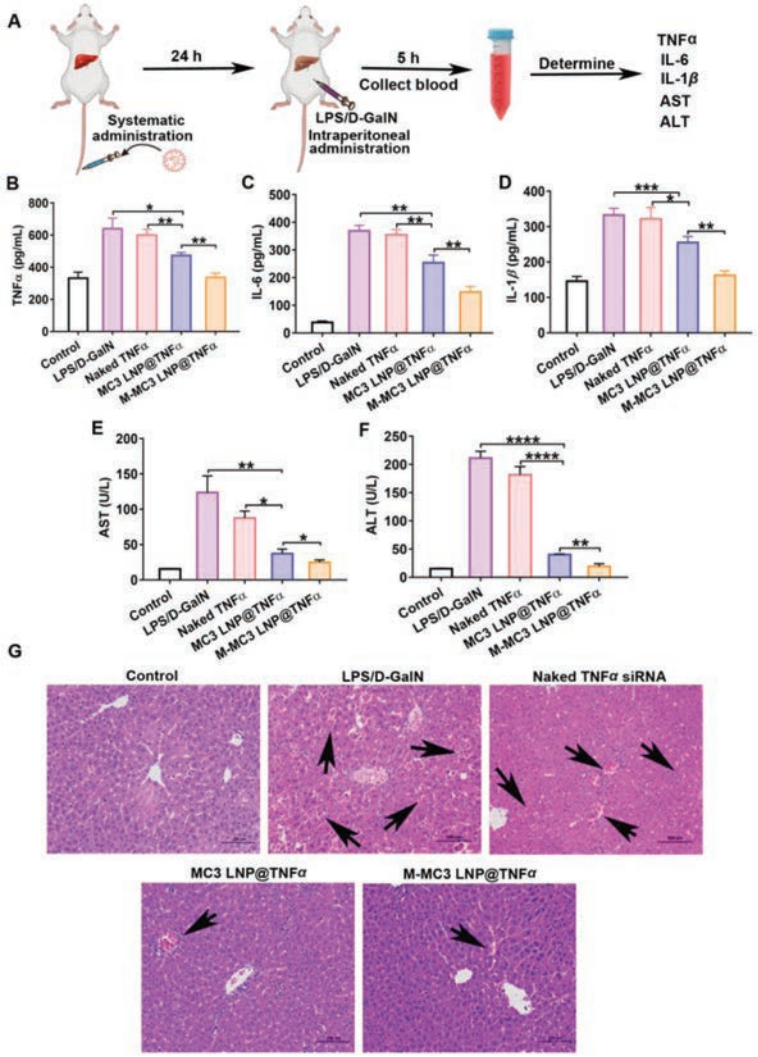

Fig. 6. The anti-inflammatory effect of M-MC3 LNP@TNFα against LPS/D-GalN-induced acute liver injury. (A) Schematic illustration of the treatment in an acute liver injury model. (B) The level of TNFα in plasma. (C) The level of IL-6 in plasma. (D) The level of IL-1β in plasma. (E) The level of aspartate aminotransferase (AST). (F) The level of alanine aminotransferase (ALT). Data are presented as mean ± SD ($n = 3$, $^{*}P < 0.05$, $^{**}P < 0.01$, $^{***}P < 0.001$, $^{****}P < 0.0001$). (G) H&E staining of liver slices in different groups (black arrow: inflammatory cell infiltration; scale bar: 100 μm).

tokines (TNFα, interleukin-6 (IL-6) and IL-1β) production to induce the activation of inflammatory response [28]. The molecular mechanism of LPS activating acute liver injury is as follows: LPS bind to LPS binding protein, promoting LPS transfer to membrane CD14 on the surface of Kupffer cells in the liver; Subsequently, the LPS signal through CD14 is mediated by Toll like receptor 4 (TLR4), resulting in activation of Kupffer cells [29]. Currently, various studies have used LPS to construct animal models of acute liver injury, mimicking the pathological process of clinical fulminant hepatic failure [1,3,30]. Therefore, the LPS play a significant role in the construction of the animal models for preclinical investigations of acute liver injury. As exhibited in Figs. S11A–E (Supporting information), the levels of asparate aminotransferase (AST), alanine aminotransferase (ALT), TNFα, IL-6 and IL-1β in mouse serum of LPS/D-GalN group were significantly higher than the normal mice group, suggesting inflammatory production of liver of mice in LPS/D-GalN group. In addition, it was found that obvious tissue damage of liver of mice in LPS/D-GalN group (Fig. S11F in Supporting information). The above results indicated that the acute liver injury animal model was successfully established.

The suppression effect of M-MC3 LNP@TNFα against acute liver injury was assessed by LPS/D-GalN-treated C57BL/6 mice. The schematic illustration of administration and establishment of acute liver injury model was exhibited in Fig. 6A. As illustrated in Figs. 6B–F, compared with naked TNFα and LPS/D-GalN group, the MC3 LNP@TNFα and M-MC3 LNP@TNFα group showed inflammatory factor secretion (TNFα, IL-6 and IL-1β) and lower liver function indicators (AST, ALT). In addition, the hematoxylin-eosin (H&E) staining results revealed that the hepatocytes of LPS/D-GalN and naked TNFα siRNA groups were observed to be necrotic, nuclear fragmentation, hemorrhage and inflammatory cell infiltration. However, only a small amount of inflammatory cell infiltration appeared in MC3 LNP@TNFα and M-MC3 LNP@TNFα groups (Fig. 6G). These results demonstrated that the MC3 LNP@TNFα and M-MC3 LNP@TNFα significantly inhibited acute liver injury. Notably, the M-MC3 LNP@TNFα exhibited better inhibition effect than MC3 LNP@TNFα (Figs. 6B–F), ascribing to the targeting ability of mannose on liver macrophages.

The biosafety of MC3 LNP@TNFα and M-MC3 LNP@TNFα was evaluated by using H&E staining. As depicted in Fig. S12 (Supporting information), compared with the control group (normal mice), no obvious histological morphology changes of main organs (heart, spleen, lung, kidney) was observed in MC3 LNP@TNFα and M-MC3 LNP@TNFα group. Hence, the H&E staining results

indicated the above-mentioned two LNPs had good biosafety *in vivo*.

In summary, a mannose-modified LNP loading TNFα-siRNA (M-MC3 LNP@TNFα) was rationally devised and fabricated for suppressing acute liver injury. *In vitro*, the M-MC3 LNP@TNFα exhibited good storage stability, higher cellular internalization efficiency and gene silencing efficiency. Additionally, the M-MC3 LNP@TNFα also showed higher accumulation in liver than that of MC3 LNP@TNFα. More importantly, on account of the binding effect of mannose ligand and receptor, the M-MC3 LNP@TNFα efficiently silenced the expression of TNFα in the liver and suppressing acute liver injury. Our findings demonstrate that the gene therapy based on active targeting LNP presents a great potential therapeutic strategy for liver-related diseases in the future.

Declaration of competing interest

The authors declare that they have no known competing financial interests or personal relationships that could have appeared to influence the work reported in this paper.

Acknowledgment

This work was financially supported by the National Key R&D Program of China (No. 2021YFA0909900).

Supplementary materials

Supplementary material associated with this article can be found, in the online version, at doi:10.1016/j.cclet.2023.108683.

References

[1] F. Ding, H. Zhang, Q. Li, et al., J. Mater. Chem. B 9 (2021) 5136.
[2] Q. Yin, X. Song, P. Yang, et al., Nanomedicine 48 (2023) 102649.
[3] H. He, N. Zheng, Z. Song, et al., ACS Nano 10 (2016) 1859–1870.
[4] S. Chu, C. Tang, C. Yin, Biomaterials 52 (2015) 229–239.
[5] P. Patel, J. Fetse, C. Lin, et al., Acta Biomater 154 (2022) 374–384.
[6] M. Kim, M. Jeong, S. Hur, et al., Sci. Adv. 7 (2021) eabf4398.
[7] C. He, L. Yin, C. Tang, et al., Biomaterials 34 (2013) 2843–2854.
[8] K. Li, M. Lu, X. Xia, et al., Chin. Chem. Lett. 32 (2021) 1010–1016.
[9] J. Zhou, L. Sun, L. Liu, et al., J. Control. Release 343 (2022) 175–186.
[10] H. Zhang, F. Ding, Z. Zhu, et al., Int. J. Pharm. 631 (2023) 122489.
[11] B. Hu, B. Li, K. Li, et al., Sci. Adv. 8 (2022) eabm1418.
[12] S. Liu, J. Liu, H. Li, et al., Biomaterials 287 (2022) 121645.
[13] D. Yin, M. Zhang, J. Chen, et al., Chin. Chem. Lett. 32 (2021) 1731–1736.
[14] H. Tanaka, Y. Sakurai, J. Anindita, et al., Adv. Drug Deliv. Rev. 154 (2020) 210–226.
[15] S. Dilliard, D. Siegwart, Nat. Rev. Mater. 8 (2023) 282–300.
[16] Y. Wang, C. Li, L. Du, et al., Chin. Chem. Lett. 31 (2020) 275–280.
[17] C. Ma, D. Zhu, W. Lin, et al., Chem. Commun. 58 (2022) 4168.
[18] S. Guo, B. Liu, M. Zhang, et al., Chin. Chem. Lett. 32 (2021) 102–106.
[19] H. Kim, A. Kim, K. Miyata, et al., Adv. Drug Deliv. Rev. 104 (2016) 61–67.
[20] N. Dammes, D. Peer, Trends Pharmacol. Sci. 41 (2020) 755–775.
[21] J. Ma, J. Zhang, L. Chi, et al., Chin. Chem. Lett. 31 (2020) 1427–1431.
[22] S. Yonezawa, H. Koide, T. Asai, Adv. Drug Deliv. Rev. 154 (2020) 64–78.
[23] Q. Wang, Z. Wang, X. Sun, et al., J. Control. Release 351 (2022) 102–122.
[24] S. Liu, Q. Cheng, Tuo. Wei, et al., Nat. Mater. 20 (2021) 701–710.
[25] A. Akinc, M. Maier, M. Manoharan, et al., Nat. Nanotechnol. 14 (2019) 1084–1087.
[26] V. Apostolopoulos, T. Thalhammer, A. Tzakos, et al., J. Drug Deliv. 2013 (2013) 869718.
[27] H. Xiong, S. Liu, T. Wei, et al., J. Control. Release 325 (2020) 198–205.
[28] J. Kang, D. Kim, J. Choi, et al., Food Chem. Toxicol. 57 (2013) 132–139.
[29] G.L. Su, Am. J. Physiol. Gastrointest. Liver Physiol. 283 (2002) G256–G265.
[30] Y. Ding, S. Zhang, Z. Sun, et al., Acta Biomater. 146 (2022) 385–395.